ELECTRICAL ENGINEERING

T 190 ――――――――――――――――――――――

ELEKTROS INŽINERIJA

Difference Approximation of DC Corona Equations

S. Pačinskis, S. Žebrauskas

Department of Theoretical Electrical Engineering, Kaunas University of Technology,
Studentų st. 48, LT-51367 Kaunas, Lithuania, phone:+370 37 300268; e-mail: stasys.zebrauskas@ktu.lt

Introduction

Corona discharge devices are widely used in electrostatic precipitation, separation of dielectric materials, electrostatic spraying, electrostatic printing, xerographic copying processes, intensification of chemical reactions, heat and mass exchange processes, textile technologies, biotechnologies, etc. The main means of theoretical investigation of corona field at the beginning of corona discharge using were analytical methods based on Deutsch's and Kaptsov's assumptions, Peek's and Townend' formulas [1-3]. Numerical computation of corona fields is the main way of research during the past thirty years. Usually two-dimension approach is used representing corona field in devices with wire emitting electrodes as plane field and the field in devices with needle electrodes representing as axially symmetric one. Finite difference [4, 5] and finite element [6-8] methods are used often for two-dimensional field computations in above mentioned cases. We prefer the finite difference method for it's simplicity. This paper is devoted to computation of direct current corona field in electrode systems with wire emitting electrodes such as wire-plate, wire-duct, a set of wires parallel to plate, a set of wires placed centrally and non-centrally between two parallel plates. The main weakness of the finite difference method is the difficulty in the construction of the computational grid. It is easy to describe boundary conditions in areas surrounding the wire if the polar coordinate system is used, on the other hand the Cartesian coordinate system should be used in areas near the plane electrodes and boundaries represented by straight lines. The computational grid in Cartesian coordinates is more preferable for easiness of boundary conditions description near the plane electrodes and for relative simplicity of the equations. In each the case the grid must be significantly finer than the wire radius to achieve the sufficient accuracy of computations. Authors [4, 5] use the regular grid. Local mesh size reducing in area near the surface of the wire is used in [4] and [6]. The problem of matching the grid lines in Cartesian coordinate system and the circular surface of the wire remains in all mentioned papers. We divide all the computational area into two subareas: irregular grid at the surface of the wire and the regular one in all other areas. For this purpose we use the difference approximation of field equations in irregular and regular grids.

Field equations

The electric field of direct current corona discharge may be represented by the system of equations consisting of Poisson's equation, equation relating the field strength E and potential V, continuity equation for current density vector J, and equation relating the vectors J and E [3]. Boundary conditions needed for the solution of field equations are the values of electrode potentials and the field strength E_0 on the surface of the wire corresponding to corona onset vorltage U_0. The continuity equation involves the derivative of space charge density ρ in general case:

$$\partial\rho/\partial t + \mathrm{div}\boldsymbol{J} = 0. \qquad (1)$$

This paper deals with stationary conditions of direct current corona field, therefore $\partial\rho/\partial t = 0$. We assume also that ion mobility b = const., as in the papers of many authors [4-8]. The phenomenon of ion diffusion is denied.

There are at least two ways for solving the system of equations of corona field. The first assumes the conversion of this system to the one non-linear differential equation [6]:

$$\left(\mathrm{divgrad}V\right)^2 + \mathrm{grad}V \cdot \left(\mathrm{divgrad}V\right) = 0. \qquad (2)$$

Equation (2) may be solved by representing it as a product of two functions, each of which depends only upon x and only upon y:

$$\Delta V + \frac{\partial V}{\partial x} \cdot \frac{\partial}{\partial x}\left(\Delta V\right) + \frac{\partial V}{\partial y} \cdot \frac{\partial}{\partial y}\left(\Delta V\right) = 0. \qquad (3)$$

Equation (3) isn't often used for corona field calculations because it can lead to unpredictable behavior of numerical system [6].

Many authors use various algorithms for the numerical solution of Poisson's and continuity equations

$$\begin{cases} \Delta V = -\rho/\varepsilon, & (4) \\ \nabla\rho\cdot\nabla V = \rho^2/\varepsilon. & (5) \end{cases}$$

Solution of these equations depends upon the method of computing (finite difference or finite element), upon initial assumptions and boundary conditions [7]. Our algorithm of solution is based on finite difference method using an iterative procedure in turn from equation (4) to equation (5).

Difference equations for irregular grid

Poisson's equation (9) for two-dimensional space contains the second derivatives with respect to x and y in Cartesian coordinate system [9]:

$$\frac{\partial^2 V}{\partial x^2} + \frac{\partial^2 V}{\partial x^2} = -\frac{\rho}{\varepsilon}. \quad (6)$$

First derivatives at the point $O(x_0, y_0)$ (Fig. 1) may be expressed through corresponding first order differences as follows:

$$V'_{Ox} = \frac{V_Q - V_S}{a_Q + a_S} = \frac{V(x_0 + a_Q, y_0) - V(x_0 - a_S, y_0)}{a_Q + a_S}, \quad (7)$$

$$V'_{Oy} = \frac{V_R - V_P}{a_R + a_P} = \frac{V(x_0, y_0 + a_R) - V(x_0, y_0 - a_P)}{a_R + a_P}. \quad (8)$$

The second derivative is the derivative of the first one,

$$V''(x_0) = \frac{V'_{Q'} - V'_{S'}}{0,5(a_Q + a_S)} =$$
$$= \frac{V'(x_0 + 0,5a_Q, y_0) - V'(x_0 - 0,5a_S, y_0)}{0,5(a_Q + a_S)}, \quad (9)$$

$$V''(y_0) = \frac{V'_R - V'_P}{0,5(a_R + a_P)} =$$
$$= \frac{V'(x_0, y_0 + 0,5a_R) - V'(x_0, y_0 - 0,5a_P)}{0,5(a_R + a_P)}. \quad (10)$$

Potential derivatives with respect to coordinate x at the points Q' and S' may be found in the same manner as at the point O:

$$V'_{Q'} = \frac{V_Q - V_O}{a_Q} = \frac{V(x_0 + a_Q, y_0) - V(x_0, y_0)}{a_Q}, \quad (11)$$

$$V'_{S'} = \frac{V_O - V_S}{a_S} = \frac{V(x_0, y_0) - V(x_0 - a_S, y_0)}{a_S}. \quad (12)$$

The second derivative with respect to coordinate x at the point O:

$$V''(x_0) = \frac{a_S V(x_0 + a_Q, y_0) + a_Q V(x_0 - a_S, y_0)}{0,5a_Q a_S \cdot (a_Q + a_S)} -$$

$$-\frac{(a_Q + a_S) V(x_0, y_0)}{0,5a_Q a_S \cdot (a_Q + a_S)}. \quad (13)$$

Potential derivatives with respect to coordinate y at the points R' and P':

$$V'_{R'} = \frac{V_R - V_O}{a_R} = \frac{V(x_0, y_0 + a_R) - V(x_0, y_0)}{a_R}, \quad (14)$$

$$V'_{P'} = \frac{V_O - V_P}{a_P} = \frac{V(x_0, y_0) - V(x_0, y_0 - a_P)}{a_P}. \quad (15)$$
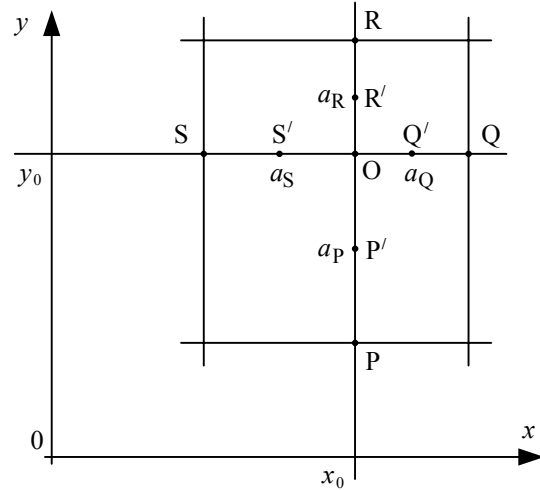

Fig. 1. Irregular grid in Cartesian coordinate system

The second derivative with respect to y at the point O:

$$V''(y_0) = \frac{a_P V(x_0, y_0 + a_R) + a_R V(x_0, y_0 - a_P)}{0,5a_P a_R \cdot (a_P + a_R)} -$$

$$-\frac{(a_P + a_R) V(x_0, y_0)}{0,5a_P a_R \cdot (a_P + a_R)}. \quad (16)$$

Substituting eqs. (13) and (16) into eq. (6) gives the difference approximation of Poisson's equation for irregular grid:

$$V(x_0, y_0) = \frac{a_Q a_S a_P a_R}{a_P a_R + a_Q a_S} \left[\frac{V(x_0 + a_Q, y_0)}{a_Q \cdot (a_Q + a_S)} + \frac{V(x_0 - a_S, y_0)}{a_S \cdot (a_Q + a_S)} + \right.$$

$$\left. + \frac{V(x_0, y_0 + a_R)}{a_R \cdot (a_P + a_R)} + \frac{V(x_0, y_0 - a_P)}{a_P \cdot (a_P + a_R)} + 2\frac{\rho(x_0, y_0)}{\varepsilon} \right], \quad (17)$$

or, in the short form,

$$V_O = k_Q V_Q + k_S V_S + k_P V_P + k_R V_R + k_\rho \rho_O; \quad (18)$$

where

$$k_Q = \frac{a_P a_R a_S}{(a_Q + a_S)(a_P a_R + a_Q a_S)}, \quad (19)$$

$$k_S = \frac{a_P a_R a_Q}{(a_Q + a_S)(a_P a_R + a_Q a_S)}, \quad (20)$$

$$k_{\mathrm{P}} = \frac{a_{\mathrm{R}} a_{\mathrm{Q}} a_{\mathrm{S}}}{(a_{\mathrm{P}} + a_{\mathrm{R}})(a_{\mathrm{P}} a_{\mathrm{R}} + a_{\mathrm{Q}} a_{\mathrm{S}})}, \qquad (21)$$

$$k_{\mathrm{R}} = \frac{a_{\mathrm{P}} a_{\mathrm{Q}} a_{\mathrm{S}}}{(a_{\mathrm{P}} + a_{\mathrm{R}})(a_{\mathrm{P}} a_{\mathrm{R}} + a_{\mathrm{Q}} a_{\mathrm{S}})}, \qquad (22)$$

$$k_{\rho} = \frac{2 a_{\mathrm{P}} a_{\mathrm{Q}} a_{\mathrm{R}} a_{\mathrm{S}}}{\varepsilon (a_{\mathrm{P}} a_{\mathrm{R}} + a_{\mathrm{Q}} a_{\mathrm{S}})}. \qquad (23)$$

Continuity equation (5) contains only of first derivatives:

$$\nabla \rho = \left[\left(\frac{\rho(x_0 + a_{\mathrm{Q}}, y_0) - \rho(x_0 - a_{\mathrm{S}}, y_0)}{a_{\mathrm{Q}} + a_{\mathrm{S}}} \right)^2 + \right.$$
$$\left. + \left(\frac{\rho(x_0, y_0 + a_{\mathrm{R}}) - \rho(x_0, y_0 - a_{\mathrm{P}})}{a_{\mathrm{P}} + a_{\mathrm{R}}} \right)^2 \right]^{0,5}, \qquad (24)$$

$$\nabla V = \left[\left(\frac{V(x_0 + a_{\mathrm{Q}}, y_0) - V(x_0 - a_{\mathrm{S}}, y_0)}{a_{\mathrm{Q}} + a_{\mathrm{S}}} \right)^2 + \right.$$
$$\left. + \left(\frac{V(x_0, y_0 + a_{\mathrm{R}}) - V(x_0, y_0 - a_{\mathrm{P}})}{a_{\mathrm{P}} + a_{\mathrm{R}}} \right)^2 \right]^{0,5}. \qquad (25)$$

Regular grid

The mesh size of regular grid is constant

$$a_{\mathrm{P}} = a_{\mathrm{Q}} = a_{\mathrm{R}} = a_{\mathrm{S}} = h. \qquad (26)$$

Coefficients $k_{\mathrm{P}}, k_{\mathrm{Q}}, k_{\mathrm{R}}, k_{\mathrm{P}}$ of Poisson's equation (18) become equal to 0,25 in this case, coefficient k_{ρ} is equal to h^2/ε. Difference approximation of Poisson's equation transforms to convenient form for regular grid [3,4],

$$V_{\mathrm{O}} = \frac{1}{4} (V_{\mathrm{P}} + V_{\mathrm{Q}} + V_{\mathrm{R}} + V_{\mathrm{S}}) + \frac{h^2}{\varepsilon} \cdot \rho_{\mathrm{O}}. \qquad (27)$$

Charge density and potential gradients in continuity equation (5),

$$\nabla \rho = \frac{1}{2h} \cdot \sqrt{(\rho_{\mathrm{Q}} - \rho_{\mathrm{S}})^2 + (\rho_{\mathrm{R}} - \rho_{\mathrm{P}})^2}, \qquad (28)$$

$$\nabla V = \frac{1}{2h} \cdot \sqrt{(V_{\mathrm{Q}} - V_{\mathrm{S}})^2 + (V_{\mathrm{R}} - V_{\mathrm{P}})^2}. \qquad (29)$$

Substituting eqs. (28) and (29) into an eq. (5) gives the difference approximation of continuity equation:

$$\rho_{\mathrm{O}} = \left[-\frac{\varepsilon}{4h^2} \sqrt{((V_{\mathrm{Q}} - V_{\mathrm{S}})^2 + (V_{\mathrm{R}} - V_{\mathrm{P}})^2} \times \right.$$
$$\left. \times \sqrt{(\rho_{\mathrm{Q}} - \rho_{\mathrm{S}})^2 + (\rho_{\mathrm{R}} - \rho_{\mathrm{P}})^2} \right]^{0,5}. \qquad (30)$$

Iterative procedure is used for numerical solving the eqs. (27) and (30).

Boundary area of irregular grid

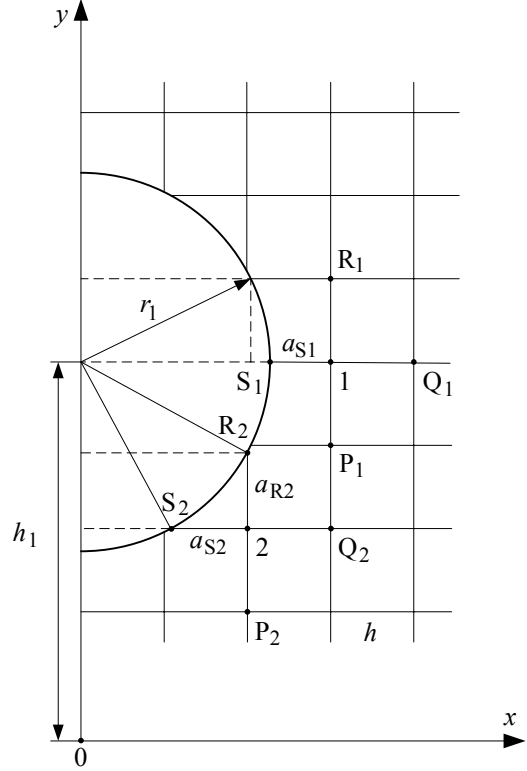Boundary area of irregular grid at the surface of wire electrode is shown in Fig. 2.

Fig. 2. Boundary area of irregular grid

There are two types of points in this area: a point $1(x_1, y_1)$ having a one irregular distance $a_{\mathrm{S}1}$, and a point $2(x_2, y_2)$ having two irregular distances $a_{\mathrm{R}2}$ and $a_{\mathrm{S}2}$ in the five-point computational scheme. Assuming that the coordinate of wire center is h_1, it's radius r_1, mesh size of regular grid h and coordinates of the points 1 and 2 may be written as $x_1 = i_1 h$, $y_1 = j_1 h$, $x_2 = i_2 h$, and $y_2 = j_2 h$, these distances may be found from geometrical relations:

$$a_{\mathrm{S}1} = x_1 - \sqrt{r_1^2 - (y_1 - h_1)^2} = i_1 h - \sqrt{r_1^2 - (j_1 h - h_1)^2}, \quad (31)$$

$$a_{\mathrm{S}2} = x_2 - \sqrt{r_1^2 - (h_1 - y_2)^2} = i_2 h - \sqrt{r_1^2 - (h_1 - j_2 h)^2}, \quad (32)$$

$$a_{\mathrm{R}2} = h_1 - \sqrt{r_1^2 - x_2^2} - y_2 = h_1 - \sqrt{r_1^2 - (i_2 h)^2} - j_2 h. \quad (33)$$

Values of computational scheme distances for points in wire boundary area laying between straight lines $x = 0$ and $y = h_1$ (Fig. 2) are given in Table 1(for $h_1 = 10,0$ mm, $r_1 = 0,1$ mm, $h = 0,02$ mm).

Table 1. Computational scheme distances for wire boundary area

x	y	a_{P}	a_{Q}	a_{R}	a_{S}
0,02	9,90	0,020	0,020	0,002	0,020
0,04	9,90	0,020	0,020	0,008	0,020
0,06	9,90	0,020	0,020	0,020	0,020
0,08	9,92	0,020	0,020	0,020	0,020
0,10	9,94	0,020	0,020	0,020	0,020
0,10	9,96	0,020	0,020	0,020	0,008
0,10	9,98	0,020	0,020	0,020	0,002

Values of coefficients $k_P - k_S$ in eq. (18) found from eqs. (19)–(22) and corresponding to the distances of Table 1 are given in Table 2. Dimensions of point coordinates x and y are given in mm in both tables.

Table 2. Values of coefficients $k_P - k_\rho$ for wire boundary area

x	y	k_P	k_Q	k_R	k_S
0,02	9,90	0,083	0,046	0,825	0,046
0,04	9,90	0,021	0,147	0,498	0,147
0,06	9,90	0,250	0,250	0,250	0,250
0,08	9,92	0,250	0,250	0,250	0,250
0,10	9,94	0,250	0,250	0,250	0,250
0,10	9,96	0,147	0,208	0,147	0,498
0,10	9,98	0,046	0,083	0,046	0,825

The sum of weight coefficients k_P, k_Q, k_R, and k_S for each point in wire boundary area is equal to 1. The smaller value of the distance a from the surface of wire causes the greater value of corresponding coefficient.

Conclusions

1. Digital approximation of DC corona field differential equations for irregular and regular grids in Cartesian coordinates is presented.
2. Values of weight coefficients of Poisson's equation for irregular grid in wire boundary area are inverse proportional to the corresponding distances from the surface of the wire.

References

1. **Pačinskis S., Žebrauskas S**. Volt-Ampere Characteristic of an Electrostatic Precipitator with Wire Electrodes // Proceedings of International Conference Electrical and Control Technologies-2006. – Kaunas: Technologija, 2006. – P. 138 –141.
2. **Bansevičius R**., **Virbalis J.A.** Distribution of Electric Field in the Round Hole of Plane Capacitor // Journal of Electrostatics. – 2006. – Vol. 64, No. 3-4. – P. 226 – 233.
3. **Žebrauskas S., Ramanauskas A.** Vienpolio vainikinio išlydžio elektrinio vėjo greičių skaičiavimas // Elektronika ir elektrotechnika. – 2002. – Nr. 5(54). – P. 70 – 75.
4. **Anagnastopoulos J., Mergeles G.** Corona Discharge Simulation in Wire-Duct Electrostatic Precipitator // Journal of Electrostatics. – 2002. – Vol. 54, No. 2. – P. 129 – 147.
5. **Caron A., Dascalescu L.** Numerical Modeling of Combined Corona-Electrostatic Fields // Journal of Electrostatics. – 2004. – Vol. 61, No. 1. – P. 43 – 55.
6. **Rafiroiu D., Munteanu C., Morar R., Meroth A., Atten P., Dascalescu L.** Computation of the Electric Field in Wire Electrode Arrangements for Electrostatic Processes Applications // Journal of Electrostatics. – 2001. – Vol. 51–52, No. 5. – P. 571 – 577.
7. **Adamiak K., Atten P.** Simulation of Corona Discharge in Point-Plane Configuration // Journal of Electrostatics. – 2004. – Vol. 61, No. 2. – P. 85 – 98.
8. **Oussalah N., Zebboud Y.** Negative Corona Computation in Air // Engineering with Computers. – 2006. – Vol. 21. – P. 296 – 303.
9. **Sadiku M.N.O.** Numerical Techniques in Electromagnetics, 2nd Ed., CRC Press Pb. – 2001. – 743 p.

S. Pačinskis, S. Žebrauskas. Difference Approximation of DC Corona Equations // Electronics and Electrical Engineering. – Kaunas: Technologija, 2007. – No. 4(76). – P. 71–74.
Methods and algorithms of direct current corona field computation are discussed. Finite difference method associated with Cartesian coordinate system is chosen for simplicity of programming and generation of computational grid. Area of computation is divided into two subareas: the area of regular grid limited by surfaces of plane electrodes and axies of symmetry, and the area of irregular grid near the surface of the corona wire. Difference approximation of Poisson's and continuity equations are given for irregular and regular grids. The values of weight coefficients of finite difference Poisson's equation for irregular grid are inverse proportional to the distances of the point from the surface of the wire, the sum of all these coefficients is equal to one. Ill. 2, bibl. 9 (in English; summaries in English, Russian and Lithuanian).

С. Пачинскис, С. Жебраускас. Конечно-разностная аппроксимация уравнений униполярного коронного разряда // Электроника и электротехника. – Каунас: Технология, 2007. – № 4(76). – С. 71–74.
Обсуждены методы и алгоритмы вычисления электрического поля униполярного коронного разряда. Из-за простоты программирования и составления сетки вычисления выбран метод конечных разностей в системе декартных координат. Расчетная область поля состоит из области регулярной сетки, ограниченной поверхностями плоских электродов и осями симметрии, и области нерегулярной сетки вблизи поверхности коронирующего электрода. Приведены разностные уравнения Пуассона и непрерывности линий плотности тока для нерегулярной и регулярной сетки. Значения коэффициентов разностного уравнения Пуассона для нерегулярной сетки обратно пропорциональны соответствующим расстояниям от поверхности коронирующего электрода при сумме всех коэффициентов равной единице. Ил. 2, библ. 9 (на английском языке; рефераты на английском, русском и литовском яз.).

S. Pačinskis, S. Žebrauskas. Vienpolio vainikinio išlydžio lygčių skirtuminė aproksimacija // Elektronika ir elektrotechnika. - Kaunas: Technologija, 2007. – Nr. 4(76). – P. 71–74.
Aptarti vienpolio vainikinio išlydžio elektrinio lauko skaičiavimo metodai ir algoritmai. Dėl programavimo ir tinklelio sudarymo paprastumo pasirinktas baigtinių skirtumų metodas naudojant dekartinių koordinačių sistemą. Skaičiuojamą lauko sritį sudaro taisyklingo tinklelio sritis, ribojama plokščiųjų elektrodų ir simetrijos ašių, ir netaisyklingo tinklelio sritis šalia vainikinio išlydžio elektrodo – laido paviršiaus. Pateiktos Poissono ir srovės tankio linijų nenutrūkstamumo skirtuminės lygtys tiek taisyklingam, tiek netaisyklingam tinkleliui. Skirtuminės Poissono lygties netaisyklingam tinkleliui svorinių koeficientų vertės yra tuo didesnės, kuo mažesni atitinkami taško atstumai iki laido paviršiaus. Kiekvienam netaisyklingo tinklelio taškui šių koeficientų suma lygi vienetui. Il. 2, bibl. 9 (anglų kalba; santraukos anglų, rusų ir lietuvių k.).